ELSEVIER

Probabilistic Engineering Mechanics 20 (2005) 158–167

PROBABILISTIC ENGINEERING MECHANICS

www.elsevier.com/locate/probengmech

Translation vectors with non-identically distributed components

Sanjay R. Arwade*

Department of Civil Engineering, The Johns Hopkins University, 202 Latrobe Hall, 3400 N. Charles Street, Baltimore, MD 12118, USA

Received 22 June 2004; received in revised form 10 January 2005; accepted 7 February 2005
Available online 20 June 2005

Abstract

A model for non-Gaussian random vectors is presented that relies on a modification of the standard translation transformation which has previously been used to model stationary non-Gaussian processes and non-Gaussian random vectors with identically distributed components. The translation model has the ability to exactly match target marginal distributions and a broad variety of correlation matrices. Joint distributions of the new class of translation vectors are derived, as are upper and lower bounds on the target correlation that depend on the target marginal distributions. Examples are presented that demonstrate the applicability of the approach to the modelling of heterogeneous material properties, and also illustrate the possible shortcomings of using second moment characterizations for such random vectors. Lastly, an outline is given of a method under development for extending the model to non-stationary, non-Gaussian random processes.

Keywords: Translation vector; Non-Gaussian vectors; Random vectors; Random processes; Non-stationary processes; Heterogeneous material properties; Crystallographic orientation

1. Introduction

Many engineering systems contain elements of uncertainty that are governed by probability rules that are not Gaussian. Examples include the wind pressure on the facade of a building, the local phase volume fraction in composite materials, and the crystallographic orientation in crystalline solids. A variety of techniques exist for generating realizations of non-Gaussian random variables, processes, and fields [1–4]. One of these techniques is the translation technique, in which non-Gaussian random quantities or functions are modelled as non-linear transformations of Gaussian random quantities [5,6]. The translation mapping has been successfully applied to random variables, vectors, and vector fields of arbitrary dimension. The purpose of this paper is to extend the translation model to random vectors that have components that are not identically distributed. The simulation of wind pressure fields is an area in which such a need has been identified, and some steps have been taken to modify the translation method for such applications [7]. Another example application of such a model would be the local volume fraction and elastic modulus fields in a random composite material. Each of these fields is in general non-Gaussian, but the fields have non-zero cross-correlation.

Non-Gaussian random variables, vectors, fields, and vector fields have wide application in essentially all engineering disciplines. For that reason, the problem of simulating such non-Gaussian random quantities has received wide attention. Two main approaches have been used in solving this problem: (1) non-linear transformations of Gaussian quantities, and (2) iterative algorithms. In both cases, the goal of the approach has most often been to match marginal distributions and second moment properties.

A common transformation technique is the translation model, details about which are given in the next section. In translation modelling of a non-Gaussian random process, for example, a non-linear transformation, based on the target marginal distribution of the process, is applied to an underlying Gaussian random process. This non-linear transformation delivers a non-Gaussian process with specified target marginal distribution. With appropriate calibration of the correlation function of the underlying Gaussian process, a specified target correlation function of the non-Gaussian process can be matched, within certain limitations.

Several versions of iterative approaches have been developed for simulating non-Gaussian random quantities.

* Corresponding author. Tel.: +1 410 516 7138; fax +1 410 516 7473.
E-mail address: srarwade@jhu.edu.

0266-8920/$ - see front matter © 2005 Elsevier Ltd. All rights reserved.
doi:10.1016/j.probengmech.2005.02.002

These approaches provide samples of non-Gaussian processes that approximately match target marginal distributions and correlation functions [1,2]. The error in the distributions and correlation functions can be made arbitrarily small by increased iteration. The advantage of these methods is their flexibility. They are able to produce approximate samples of certain non-Gaussian processes that cannot be modelled as translation processes. The disadvantage is the computational expense of the iterative procedure and the approximate nature of the agreement with target distributions and correlation functions.

To date, translation modelling has been applied to scalar valued random processes and fields, random vectors with identically distributed components, and vector random processes and fields with identically distributed components. This paper extends the model to random vectors with non-identically distributed components. It is indicated that this addition to the model may provide the ability to model non-stationary non-Gaussian random processes and fields.

First, a brief review of the translation model is given. Next the mathematical extension of the model to random vectors with non-identically distributed components is presented. The paper closes with three example applications, one an idealized example to illustrate the applicability, and two examples in which actual experimental data are modelled using the extended translation model. The examples are taken from experimental measurements of local random material properties in polycrystalline aluminum and F-Actin polymer suspensions. Finally an approach to the simulation of non-Gaussian non-stationary processes is given in outline form.

2. The translation model

The goal of the translation model is to provide an efficient method for simulating non-Gaussian random vectors and fields with specified target marginal distribution and correlation function. Since the topic of this paper is non-Gaussian random vectors, the translation model is now described briefly for the case of random vectors.

Let $\mathbf{Z} \in \mathbb{R}^d$ be a non-Gaussian random vector. The components $\{Z_i\}$ of $\mathbf{Z}$ have marginal cumulative distribution function (cdf) $F(z)$, marginal probability density function $f(z)$, and the covariance matrix $\mathbf{c}$ defined by $\mathbf{c} = E[(\mathbf{Z}-\boldsymbol{\mu})(\mathbf{Z}-\boldsymbol{\mu})^{\mathrm{T}}]$ where $E[\cdot]$ is the expectation operator. The components of the scaled covariance matrix $\boldsymbol{\xi}$ of $\mathbf{Z}$ are $\xi_{ij} = c_{ij}/\sqrt{c_{ii}c_{jj}}$. The translation model treats the random vector $\mathbf{Z}$ as a non-linear transformation of a Gaussian random vector $\mathbf{Y} \in \mathbb{R}^d$. The transformation is given by

$$Z_i = g(Y_i) = F^{-1} \circ \Phi(Y_i) \tag{1}$$

where $\Phi(\cdot)$ is the standard (mean zero, unit variance) Gaussian cdf, and $\{Y_i\}$ are the components of $\mathbf{Y}$. Exact expressions for the joint pdfs and cdfs of $\mathbf{Z}$ have been derived [6].

The underlying Gaussian vector $\mathbf{Y}$ has components that are standard Gaussian random variables, and correlation matrix $\mathbf{r}_{\mathrm{g}} = E[\mathbf{Y}\mathbf{Y}^{\mathrm{T}}]$ that is equal to the scaled covariance matrix $\boldsymbol{\xi}_{\mathrm{g}} = \mathbf{r}_{\mathrm{g}}$. The components of $\boldsymbol{\xi}$ are given in terms of the components of $\boldsymbol{\xi}_{\mathrm{g}}$ by

$$\mu_i\mu_j + \sqrt{c_{ii}c_{jj}}\xi_{ij} = \int_{-\infty}^{\infty}\int_{-\infty}^{\infty} g(u)g(v)\phi(u,v;\xi_{g,ij})\mathrm{d}u\ \mathrm{d}v \tag{2}$$

where $\phi(\cdot,\cdot;\xi)$ is the bivariate Gaussian density function with correlation coefficient ξ. This expression demonstrates that the non-linear transformation of Eq. (1) distorts the correlation, so that $\boldsymbol{\xi} \neq \boldsymbol{\xi}_{\mathrm{g}}$. It can be shown that $\xi_{\mathrm{g},ij} = 0 \Rightarrow \xi_{ij} = 0$ and $\xi_{\mathrm{g},ij} = 1 \Rightarrow \xi_{ij} = 1$. The implication $\xi_{\mathrm{g},ij} = -1 \Rightarrow \xi_{ij} = -1$ does not, however, hold. The lower bound on any component ξ_{ij} of $\boldsymbol{\xi}$ is given by

$$\xi^* = \frac{E[g(U)g(-U)] - E[g(U)]^2}{E[g(U)^2] - E[g(U)]^2} \tag{3}$$

where U is a standard Gaussian random variable that serves as a dummy variable. When $g(\cdot)$ is an odd function $\xi^* = -1$, otherwise $\xi^* > -1$. It is, therefore not possible to simulate random vectors for which $g(\cdot)$ is not odd, and for which $\xi_{ij} < \xi^*$ for some index pair (i, j).

3. Non-identically distributed components

Consider now a random vector $\mathbf{Z} \in \mathbb{R}^d$ that has components with marginal cdfs $\{F_i(z)\}$. If $F_i(z) = F_j(z)\ \forall i, j \in [1,d]$, then the vector can be modelled as a standard translation vector as described in the previous section. More generally, when all the cdfs $\{F_i(z)\}$ are distinct, it is now shown how $\mathbf{Z}$ can be modelled by the translation mapping

$$Z_i = g_i(Y_i) = F_i^{-1} \circ \Phi(Y_i) \tag{4}$$

where $\{Y_i\}$ are the components of the standard Gaussian vector $\mathbf{Y}$. This transformation amounts to a standard translation model for each of the components of $\mathbf{Z}$. The target marginal distribution functions are matched exactly since

$$\begin{aligned} P(Z_i \le z) &= P(F_i^{-1} \circ \Phi(Y_i) \le z) = P(Y_i \le \Phi^{-1} \circ F_i(z)) \\ &= F_i(z). \end{aligned} \tag{5}$$

The joint cdf of $\mathbf{Z}$ is given by

$$F(\mathbf{z}) = \Phi(\mathbf{y}) \tag{6}$$

where $\Phi(\cdot)$ is the d-dimensional joint Gaussian cdf, and $\mathbf{y}$ has components $y_i = \Phi^{-1} \circ F_i(z_i)$. The joint pdf is

$$f(\mathbf{z}) = \phi(\mathbf{y}) \prod_{r=1}^{d} \frac{f_r(z_r)}{\phi(y_r)}$$

$$= \frac{1}{\sqrt{(2\pi)^d \det(\boldsymbol{\xi}_g)}} \exp\left(-\frac{1}{2}\mathbf{y}^T \boldsymbol{\xi}_g^{-1} \mathbf{y}\right) \prod_{r=1}^{d} \frac{f_r(z_r)}{\phi(y_r)}. \quad (7)$$

where $\phi(\cdot)$ is the Gaussian pdf.

The scaled covariance matrix $\boldsymbol{\xi}$ of $\mathbf{Z}$ is defined in terms of the functions $\{g_i(\cdot)\}$, and the correlation $\boldsymbol{\xi}_g$ of the underlying Gaussian vector $\mathbf{Y}$ as

$$\mu_i\mu_j + \sqrt{c_{ii}c_{jj}}\xi_{ij} = \int_{-\infty}^{\infty}\int_{-\infty}^{\infty} g_i(u)g_j(v)\phi(u, v; \xi_{g,ij})\mathrm{d}u\ \mathrm{d}v, \quad (8)$$

which, as in the case where $\mathbf{Z}$ has identically distributed components, introduces a distortion in the correlation between $\mathbf{Y}$ and $\mathbf{Z}$. It is emphasized at this point that, for $\mathbf{Z}$ to be modeled as a translation vector, $\boldsymbol{\xi}_g$, the correlation matrix of the underlying Gaussian vector must be non-negative definite. If this is not the case, the correlation matrix and marginal distributions of $\mathbf{Z}$ are non-compatible, and the translation model cannot be used. The main contribution of this paper is to investigate this correlation distortion, particularly identifying the limitations on the target scaled covariance $\boldsymbol{\xi}$.

Each component of the non-Gaussian scaled covariance depends solely upon the corresponding component of the Gaussian scaled covariance such that $\xi_{ij} = h_{ij}(\xi_{g,ij})$ where the form of $h_{ij}(\cdot)$, called the correlation distortion function, is determined by the marginal distributions of Z_i and Z_j through $g_i(\cdot)$ and $g_j(\cdot)$. It is first shown that $h_{ij}(\cdot)$ is a non-decreasing function.

The Price theorem [8] gives

$$\frac{\mathrm{d}}{\mathrm{d}\xi_{g,ij}} h_{ij}(\xi_{g,ij}) = \frac{\partial \xi_{ij}}{\partial \xi_{g,ij}} = \frac{1}{\sqrt{c_{ii}c_{jj}}} E\left[\frac{\mathrm{d}}{\mathrm{d}U} g_i(U) \frac{\mathrm{d}}{\mathrm{d}U} g_j(U)\right] \quad (9)$$

and since the functions $\{g_i(\cdot)\}$ are non-decreasing since the marginal cdfs $\{F_i(\cdot)\}$ are non-decreasing functions, the right-hand side of Eq. (9) is always non-negative, and ξ_{ij} is non-decreasing in $\xi_{g,ij}$.

Since $h_{ij}(\cdot)$ is a non-decreasing function and $-1 \le \xi_{g,ij} \le 1$, ξ_{ij} must be bounded by

$$h_{ij}(-1) \le \xi_{ij} \le h_{ij}(1). \quad (10)$$

The functions h_{ij} also satisfy $h_{ij}(0) = 0$ so that $\xi_{g,ij} = 0 \Rightarrow \xi_{ij} = 0$. This holds since, when $\xi_{g,ij} = 0$ the Gaussian random variables Y_i and Y_j are independent, and Eq. (8) can be rewritten as

$$\xi_{ij} = \left[\int_{-\infty}^{\infty} g_i(u)\phi(u)\mathrm{d}u \int_{-\infty}^{\infty} g_j(v)\phi(u)\mathrm{d}v - \mu_i\mu_j\right](c_{ii}c_{jj})^{-1/2} = 0. \quad (11)$$

When $\xi_{g,ij} = -1$, the bivariate Gaussian pdf $\phi(u, v; -1)$ takes non-zero values only for $u = -v$, and evaluation of $h_{ij}(-1)$ yields

$$\mu_i\mu_j + \sqrt{c_{ii}c_{jj}}\xi_{ij}^{\min} = \int_{-\infty}^{\infty} g_i(u)g_j(-u)\phi(u)\mathrm{d}u \quad (12)$$

and

$$\xi_{ij}^{\min} = \frac{E[g_i(U)g_j(-U)] - E[g_i(U)]E[g_j(U)]}{\sqrt{(E[g_i(U)^2] - \mu_i^2)(E[g_j(U)^2] - \mu_j^2)}} \quad (13)$$

where U is again a dummy Gaussian variable and $\xi_{ij}^{\min}$ is the lower bound on ξ_{ij}, and is analogous to the bound given in Eq. (3). Eq. (13) reduces to Eq. (3) when $g_i(U) = g_j(U)$. The upper bound is found by evaluating $h_{ij}(1)$, for which $\phi(u, v; 1)$ takes non-zero values only along the line $u = v$. The upper bound is

$$\mu_i\mu_j + \sqrt{c_{ii}c_{jj}}\xi_{ij}^{\max} = \int_{-\infty}^{\infty} g_i(u)g_j(u)\phi(u)\mathrm{d}u, \quad (14)$$

or

$$\xi_{ij}^{\max} = \frac{E[g_i(U)g_j(U)] - E[g_i(U)]E[g_j(U)]}{\sqrt{(E[g_i(U)^2] - \mu_i^2)(E[g_j(U)^2] - \mu_j^2)}} \quad (15)$$

which reduces to $\xi_{ij}^{\max} = 1$ when $g_i(U) = g_j(U)$.

One final property of the correlation distortion function $h_{ij}(\cdot)$ is that it is an odd function if either or both of $g_i(\cdot)$ or $g_j(\cdot)$ are themselves odd. The definition of $h_{ij}(\xi)$, as given in Eq. (8) is

$$h_{ij}(\xi) = \left[\int_{-\infty}^{\infty}\int_{-\infty}^{\infty} g_i(u)g_j(v)\phi(u, v; \xi)\mathrm{d}u\ \mathrm{d}v - \mu_i\mu_j\right] \times (c_{ii}c_{jj})^{-1/2}. \quad (16)$$

Substitution of $-\xi$ as the argument gives

$$h_{ij}(-\xi) = \left[\int_{-\infty}^{\infty}\int_{-\infty}^{\infty} g_i(u)g_j(v)\phi(u, v; -\xi)\mathrm{d}u\ \mathrm{d}v - \mu_i\mu_j\right] \times (c_{ii}c_{jj})^{-1/2}, \quad (17)$$

in which the change of variables $v = -v$ can be applied without altering the integrals, yielding

$$h_{ij}(-\xi) = \left[\int_{-\infty}^{\infty}\int_{-\infty}^{\infty} g_i(u)g_j(-v)\phi(u, -v; \xi)\mathrm{d}u\ \mathrm{d}v - \mu_i\mu_j\right] \times (c_{ii}c_{jj})^{-1/2} \quad (18)$$

which, if $g_j(v) = -g_j(-v)$, implying that $E[g_j(V)] = 0$, becomes

$$h_{ij}(-\xi) = -\left[\int_{-\infty}^{\infty}\int_{-\infty}^{\infty} g_i(u)g_j(v)\phi(u, -v; \xi)\mathrm{d}u\ \mathrm{d}v\right](c_{ii}c_{jj})^{-1/2} = -h_{ij}(\xi), \quad (19)$$

so that $h_{ij}(\xi)$ is odd. The above steps can be repeated for the case where $g_i(\cdot)$ is odd since the integration variables can be interchanged freely, and also for the case where both $g_i(\cdot)$ and $g_j(\cdot)$ are odd. When at least one of $g_i(\cdot)$ and $g_j(\cdot)$ are odd, the upper and lower bounds on ξ_{ij} are equal and opposite so that $\xi_{ij}^{\min} = -\xi_{ij}^{\max}$.

The calculation of the correlation distortion function, the main feature of the translation approach to modeling non-Gaussian random vectors, can be computationally somewhat time consuming. If data are available, several other approaches exist for generating samples that match the target marginal distributions and second moment properties of the non-Gaussian data. One approach would be to simply convert the non-Gaussian data $\mathbf{z}$ to the Gaussian space using the inverse transformation of Eq. (4), and then estimate the Gaussian correlation matrix from the transformed data. This approach yields equivalent results to the translation model in the case where data are available with the target marginal distributions and desired target correlation structure. In many cases, however, it is desired to generate non-Gaussian samples with specified marginal distributions and correlations that may not correspond to an available data set. In this case, the correlation distortion function can be used to generate data with any compatible correlation structure. A similar approach would be to transform the non-Gaussian data by, for example, the inverse modal decomposition $\mathrm{X} = \sqrt{\mathrm{d}}^{-1}\mathrm{v}^{-1}\mathrm{Z}$, where $\mathbf{d}$ is a diagonal matrix containing the eigenvalues of $\boldsymbol{\xi}$, and $\mathbf{v}$ the matrix of corresponding eigenvectors. This transformation yields a non-Gaussian vector $\mathbf{X}$ with uncorrelated (but not necessarily independent) components. By generating independently the uncorrelated components of $\mathbf{X}$ and retransforming into the correlated non-Gaussian space, satisfactory matching of the target correlation and marginal distributions can be obtained. It should be noted that independent component generation immediately introduces an error since lack of correlation does not imply independence in the non-Gaussian space. This approach could, however, be highly efficient for cases where the random vector is of relatively small dimension, and where data are available. Again, however, it does not provide the flexibility of the translation approach in generating samples with arbitrary compatible correlation and marginal distributions. The translation approach is particularly appropriate if the sensitivity of some system response to parameters of the marginal distributions or correlation structure is desired.

4. Examples

Three example applications are now given. In the first, a two-dimensional random vector with one exponential and one cubic form component is simulated using the translation model. The second presents simulation of the crystallographic orientation of a polycrysalline material, and in the third the elasticity and viscosity of a polymer suspension are simulated.

The translation model provides a means for exact matching of target marginal distributions and correlation coefficients that is highly efficient. Once the correlations of the underlying Gaussian have been calibrated, the steps for non-Gaussian simulation are (1) Gaussian simulation, and (2) translation, each of which can be accomplished in seconds per sample for random vectors of up to several thousand components on a desktop computer. The time consuming part of the simulation scheme is the calculation of the correlation distortion functions $h_{ij}(\cdot)$, which must be done, typically, by numerically solving Eq. (8). For a random vector with n components, each with a different marginal distribution, there exist $(n^2-n)/2$ such functions, since $h_{ij}(\cdot) = h_{ji}(\cdot)$. In the author's experience, the correlation distortion functions tend to be quite smooth, and thus a sufficiently accurate representation of $h_{ij}(\xi_{g,ij})$ can be obtained by evaluating Eq. (8) at approximately 20 values of $\xi_{g,ij}$ and interpolating these values. Thus, approximately $10(n^2-n)$ evaluations of Eq. (8) are required to calibrate the translation model of an n-dimensional random vector. On a desktop computer, a typical evaluation of Eq. (8) takes in the order of 1 s. Vectors of dimension up to approximately 20 can be calibrated in under 1 h of computation time. A vector of dimension 100 would take approximately 1 day of computation time to calibrate. While these times are long, the calibration has to be done only once for each set of marginal distributions. Arbitrarily many samples can then be generated rapidly with specified target correlation matrix. Additionally, if the marginal distributions of the components are related to one another and can be parametrized (for example, a family of beta distributions), the calibration time can be further reduced. The translation model is primarily applicable to those situations in which it is desirable to be able to vary the target correlation matrix of the random vector to be simulated.

4.1. Exponential-cubic form random vectors

Let $\mathbf{Z} \in \mathbb{R}^2$ be a random vector which is to be simulated using a translation model. The component Z_1 is an exponential random variable with parameter $\lambda = 1$, and Z_2 is a random variable of cubic form. The marginal cdfs of $\mathbf{Z}$ are $F_1(z) = 1 - \exp(-z)$ and $F_2(z) = \Phi(\mathrm{sign}(z)|z|^{1/3})$, and the functions

$$g_1(y) = -\log(1 - \Phi(Y)), \quad g_2(y) = Y^3 \tag{20}$$

define the translation mapping.

The bounding values $\xi_{12}^{\min}$ and $\xi_{12}^{\max}$ are calculated by numerical integration of Eqs. (13) and (15) and yield

$$-0.75 \le \xi_{12} \le 0.75. \tag{21}$$

The correlation distortion function $h_{12}(\xi_{g,12})$, computed by numerical integration of Eq. (8), is shown in Fig. 1 and

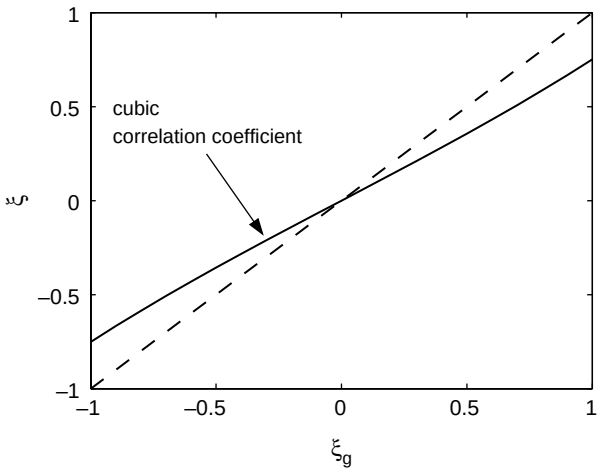

Fig. 1. Correlation distortion function for a two-dimensional non-Gaussian vector with one exponential component and one cubic form component. Function calculated by numerical integration of Eq. (8).

demonstrates the antisymmetry arising from the fact that the cubic form has an antisymmetric inverse cdf. This example illustrates that non-identically distributed components of random translation vectors need not be perfectly correlated even when the underlying Gaussian components are perfectly correlated.

To generate realizations of a two-dimensional non-Gaussian random vector with marginal distributions $F_1(z)$ and $F_2(z)$ as defined above, and with target correlation coefficient $\xi_{12}=0.5$, the correlation coefficient of the underlying Gaussian is computed by iteratively solving Eq. (8) to obtain $\xi_{g,12}=0.69$. Fig. 2 shows side by side scatter plots of 1000 independent realizations of the underlying Gaussian and the translation vector.

4.2. Crystallographic orientation

The rotational position of the periodic lattice making up crystalline solids is defined by the crystallographic orientation. The orientation is perhaps the most important microstructural parameter for the analysis of crystalline materials. Studies of polycrystalline behavior often use the orientation distribution function (ODF) to characterize the material [9–11]. Recently, models in which the orientation of individual grains is represented explicitly have been developed [12]. In any study in which Monte Carlo simulation is to be used to investigate the behavior of crystalline materials, a necessity is the ability to generate realizations of the orientation.

The orientation has many possible representations, one of which is the standard Euler angle representation [13] in which the orientation is represented by the three angles (ϕ_1, Φ, ϕ_2). In the random vector context of this paper this notation is modified so that the orientation is given by the random vector $\mathbf{\Psi}=[\Psi_1, \Psi_2, \Psi_3]^{\mathrm{T}}$ where $\mathbf{\Psi}_1=\phi_1$, $\mathbf{\Psi}_2=\mathbf{\Phi}$, and $\mathbf{\Psi}_3=\phi_2$. This example shows how the orientation can be modelled as a translation vector with non-identically distributed components.

Experimental measurement of the orientation at 14,012 points on the surface of a 540 μm×540 μm sample of AL2024 containing approximately 120 grains yields the marginal histograms for the Euler angles shown in Fig. 3 [14]. Fig. 4 shows scatter plots of the random pairs (Ψ_1, Ψ_2), (Ψ_1, Ψ_3), and (Ψ_2, Ψ_3) along with their calculated correlation coefficients. Notable features of Figs. 3 and 4 are the highly non-Gaussian nature of the data and the fact that the Euler angle pairs of Fig. 4 appear to exist only in isolated regions of the orientation space. This last fact indicates that simulation of the orientation which matches statistical properties only up to second moment may be insufficient.

The correlation distortion functions $h_{ij}(\xi_{g,ij})$, $i, j=1, 2, 3$ are calculated numerically, and are shown in Fig. 5. The correlation distortion functions show that perfect correlation cannot be achieved between the random Euler angles. The distortion is maximized near $\xi_{g,ij}=-1$ and $\xi_{g,ij}=1$ for all functions. The maximum and minimum values are given in Table 1 and show a significant maximum distortion of 0.24.

To generate realizations of the orientation vector which match the second moment properties and marginal

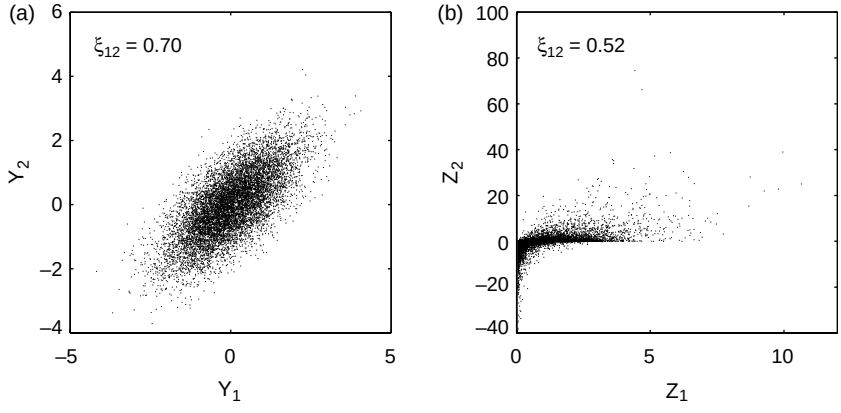

Fig. 2. Scatter plots of 10,000 independent realizations of (a) Gaussian vector **Y** and (b) non-Gaussian vector **Z** generated to match target correlation coefficient $\xi_{12}=0.5$.

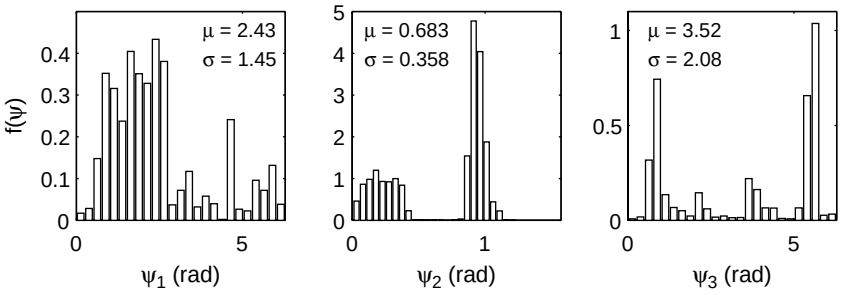

Fig. 3. Marginal histograms of Euler angles showing also the mean and standard deviation of each.

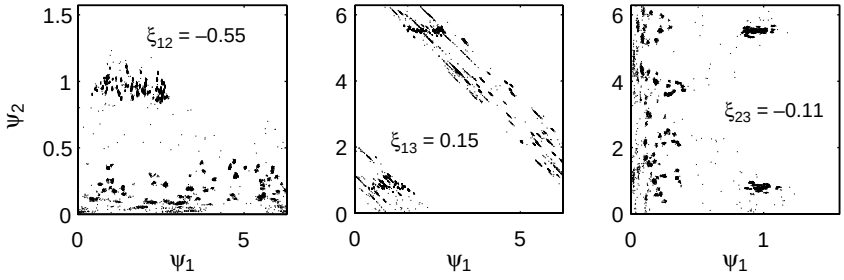

Fig. 4. Scatter plots of Euler angle pairs.

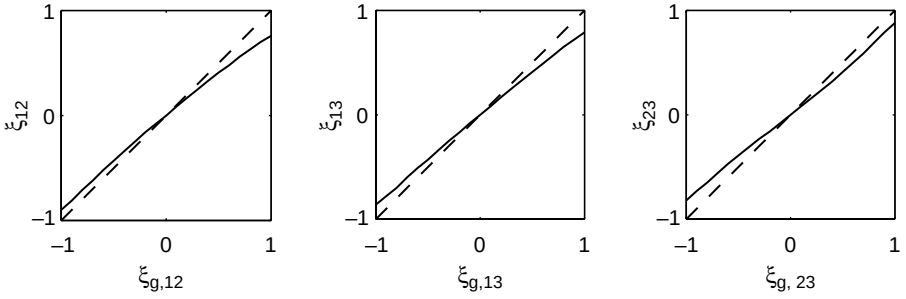

Fig. 5. Correlation distortion functions for Euler angle pairs.

distributions of the data, two steps are required. First, numerical approximations of the inverse marginal cdfs are estimated from the data. Second, the appropriate correlation matrix for the underlying Gaussian vector **Y** is computed from the estimated correlation distortion functions shown in Fig. 5. The scaled covariance matrix of the orientation vector **Z**, estimated from the data, is

$$\xi = \begin{bmatrix} 1 & -0.55 & 0.15 \\ -0.55 & 1 & -0.11 \\ 0.12 & -0.11 & 1 \end{bmatrix}. \tag{22}$$

The corresponding correlation matrix of the underlying Gaussian random vector **Y**, computed from the functions of Fig. 5 is

$$\xi_g = \begin{bmatrix} 1 & -0.62 & 0.18 \\ -0.62 & 1 & -0.14 \\ 0.18 & -0.14 & 1 \end{bmatrix}. \tag{23}$$

Using the numerical cdfs and correlation matrix of Eq. (23), 10,000 independent translation vectors are generated that match the marginal distributions. The scatter plots of Fig. 6 show that the joint distribution of pairs of orientaion components are not necessarily well matched, although the target correlation coefficients are met satisfactorily. The sample correlation coefficients are estimated to be −0.53, 0.15, and −0.11 which compare well to the target correlation coefficients of −0.55, 0.15, −0.11. The scatter plot of (ψ_1, ψ_2) compares reasonably well with its experimental target, but the plot of (ψ_1, ψ_2) is a very poor match to the target. Inspection of Fig. 4 reveals that the joint pdf of (ψ_1, ψ_2) has a banded structure. Such a structure

Table 1
Values of ξ_{ij}^{max} and ξ_{ij}^{min} for Euler angle data

Euler angle pair	(Φ_1, Φ_2)	(Φ_1, Φ_3)	(Φ_2, Φ_3)
ξ_{ij}^{min}	−0.90	−0.86	−0.82
ξ_{ij}^{max}	0.76	0.79	0.88

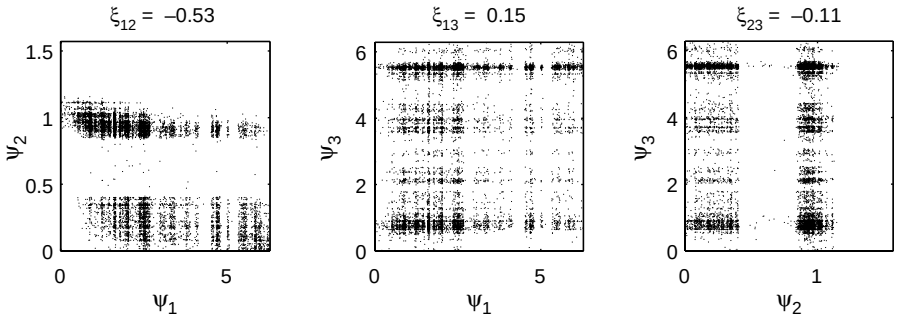

Fig. 6. Scatter plots of component pairs of simulated orientation vectors. Compare to experimental measurements in Fig. 4.

cannot be adequately captured by only the marginal histograms and second moment properties.

The structure of Fig. 4 can be simplified, however, by accounting for the periodicity of the Euler angles. The (ψ_1, ψ_2) values in the lower left-hand corner of the plot can be shifted in the ψ_1 direction by 2π without changing the physical orientation. This shifted scatter plot is shown in Fig. 7 where a much simpler structure is observed. The transformation applied to Euler angle ψ_1 alters the correlation distortion function so that the values of Fig. 5 cannot be used directly. For the transformed Euler angles, a Gaussian correlation of 0.99 is calculated to yield the target correlation coefficient of 0.98. The results of 10,000 independent realizations of the transformed Euler angle pairs are shown in Fig. 8a. The target correlation coefficient is matched successfully, and the match to the structure of the joint pdf is significantly improved, though perhaps only marginally satisfactory. An alternative approach to simulating these data would be to treat the random variables of interest as Φ_1, Φ_2, and $\Phi_1+\Phi_3$, taking advantage of the nearly linear relationship between Φ_1 and Φ_3. Such an approach would be likely to yield superior results to even the second simulation method shown here.

Fig. 8b shows the retransformed results of this simulation, and demonstrates that even pdf structures which cannot be completely characterized by their second moment properties can be modelled to a reasonable degree of accuracy using translation vectors. It must be emphasized however, that the inaccuracy of the simulated joint distribution is a major limitation in using second moments and marginal distributions as the target values of a non-Gaussian simulation.

4.3. Viscoelastic properties of F-Actin

A novel method for measuring the local viscoelastic properties of soft complex materials at the microscale has recently been developed. The experimental technique [15, 16] consists of introducing microscopic spherical beads into the subject material and tracking the position of the microspheres over time. Tracking the bead position allows determination of the elasticity and viscosity constants of the material.

The data obtained for this study consist of measurements of the local elastic and viscous material properties in a suspension of the filamentous protein F-Actin. The elastic modulus (E) and viscosity (ν) are obtained for 142 microbeads placed in the suspension. The marginal histograms and joint scatter plot of the data are shown in Fig. 9. The material properties have notably different marginal distributions and a correlation coefficient of 0.48.

The different marginal distributions of the elasticity and viscosity lead to a significant correlation distortion which reaches its extremes at $h_{12}(-1)=-0.57$ and $h_{12}(1)=0.92$ (Fig. 10). The correlation distortion is larger for negative correlations, but is also significant for positive correlation. To match the target correlation coefficient of 0.48, the function of Fig. 10 specifies a Gaussian correlation coefficient of 0.57. The scatter plot of 142 simulated random translation vectors is shown in Fig. 11 and indicates a satisfactory match to the target joint distribution and correlation coefficient. The joint scatter plot appears to agree well with that of Fig. 9.

5. Non-stationary processes

The above examples show that the translation model for random vectors with non-identically distributed

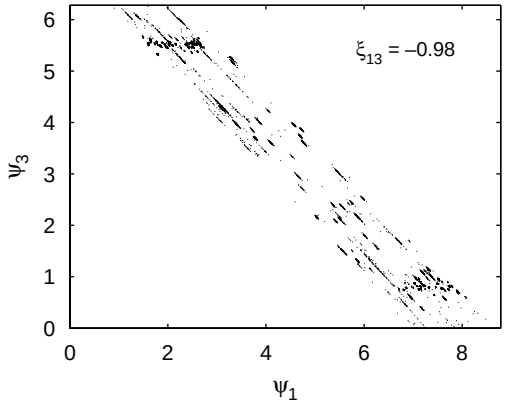

Fig. 7. Scatter plot of (ψ_1, ψ_3) with ψ_1 values shifted to reveal banded structure of joint pdf.

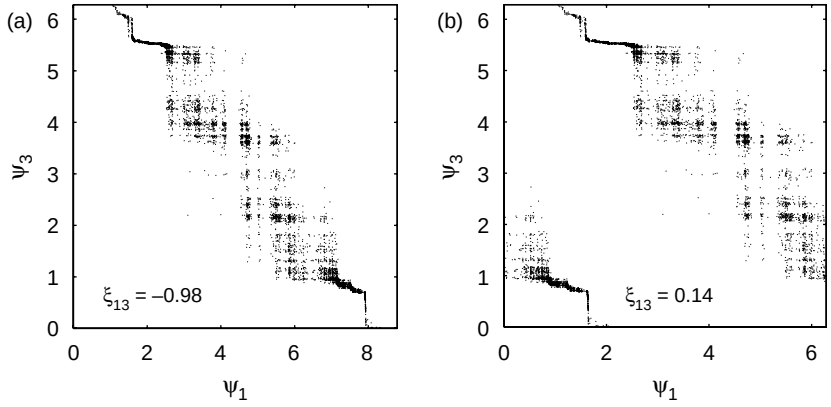

Fig. 8. Scatter plot of (ψ_1, ψ_3) with ψ_1 values shifted to reveal banded structure of joint pdf.

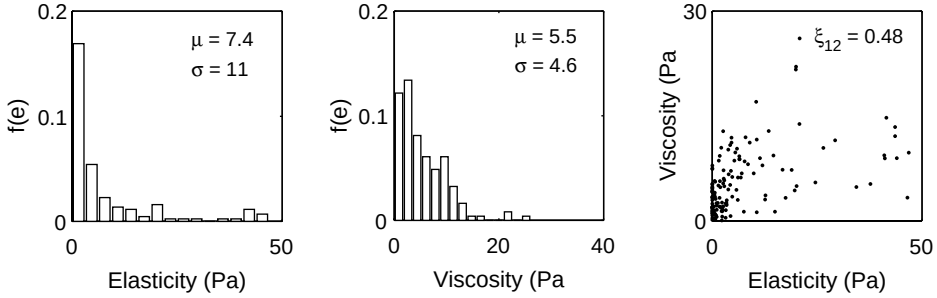

Fig. 9. Marginal histograms and scatter plot of elasticity and viscosity measurements of F-Actin obtained by the multiple particle tracking method.

components can be used to model a broad range of physically meaningful random quantities. Current research seeks to extend this translation model for application to non-stationary, non-Gaussian random processes. An outline of the approach is given here to indicate the possibility, while a full description will follow in a forthcoming publication. One of the considerations made in the ongoing research is the comparison of application of translation processes to the modeling of nonstationary processes with previously successful efforts at using the Karhunen–Loeve (KL) expansion in an iterative framework to simulate non-stationary processes [17]. While the iterative KL approach has great flexibility, it is conjectured that the translation approach may prove more efficient for certain classes of processes. Another significant comparison must be made with the performance of wavelet and evolutionary specrum based methods for simulating non-stationary processes [18,19].

Let $Z(t)$ be a non-Gaussian random process with marginal cdf $F(z, t)$ which is a function of time since the process is non-stationary. The correlation function of $Z(t)$ is denoted $r(t, t+\tau)$ and the scaled covariance function is denoted $\xi(t, t+\tau)$. This non-stationary non-Gaussian random process can be modelled by the translation

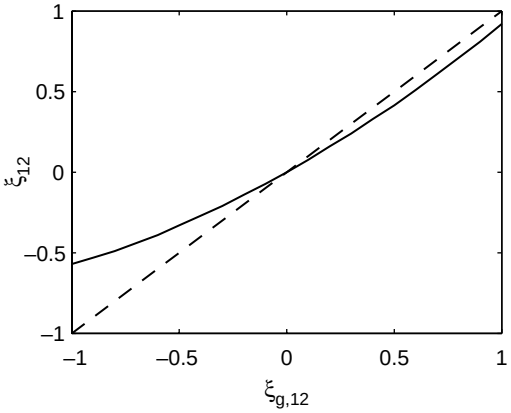

Fig. 10. Correlation distortion for a two-dimensional random translation vector modelling the elasticity and viscosity of an F-Actin suspension.

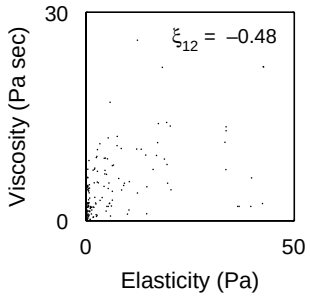

Fig. 11. Marginal histograms and scatter plot of simulated elasticity–viscosity random vectors.

$$Z(t) = F_t^{-1} \circ \Phi(Y(t)) = g_t(Y(t)) \tag{24}$$

where F_t^{-1} is the inverse marginal cdf of $Z(t)$, $\Phi(\cdot)$ is the standard Gaussian cdf and $Y(t)$ is a Gaussian random process with mean zero, unit variance, and correlation function $\xi_g(t, t+\tau)$. Such a transformation exactly matches the target, non-stationary, marginal distribution of $Z(t)$. The correlation function of $Z(t)$ is given in terms of $\xi_g(t, t+\tau)$ according to

$$\mu(t)\mu(t+\tau) + \sigma(t)\sigma(t+\tau)\xi(t, t+\tau) = \int_{-\infty}^{\infty}\int_{-\infty}^{\infty} g_t(u)g_{t+\tau}\phi(u, v; \xi_g(t+\tau))\mathrm{d}u\ \mathrm{d}v \tag{25}$$

The major complication in this approach is that the correlation distortion function $\xi(t, t+\tau) = h(t, t+\tau, \xi_g(t, t+\tau))$ given by Eq. (25) is now a function of three parameters, rather than just the correlation function of the underlying Gaussian random process $Y(t)$. Thus, in order to calibrate the correlation function of the underlying Gaussian random process, a very large number of solutions to Eq. (25) must be computed. For example, in estimating the correlation distortion function for a bivariate random vector, as in example 4.3, a reasonable approximation can be obtained by evaulating $h_{12}(\xi_g)$ at $\xi_g = [-1, -0.9, \ldots, 1]$ requiring 21 evaluations of Eq. (8). This can typically be performed in a several minutes on a desktop PC. On the other hand, if a non-Gaussian random process is to be calibrated for sample length of 100 s, and a time discretization of the correlation functions of 1 s is found to be acceptable, 210,000 evaluations of Eq. (25) are necessary, which is in general prohibitive. It may be possible to overcome this complication by appropriate parametrization of the time varying marginal distributions $F(z, t)$. A study of this approach for the simulation of functionally graded materials is currently ongoing, and will address many of these issues.

6. Conclusion

The translation model for non-Gaussian random vectors has been extended to model those non-Gaussian random vectors that have non-identically distributed components. The model is able to simulate random vectors with a broad range of marginal distribution functions and correlation matrices, matching the target values exactly in most cases. Exact expressions are derived for the joint distribution of the non-Gaussian vectors, and for the correlation matrix of the non-Gaussian vector in terms of the correlation matrix of the underlying Gaussian. Upper and lower bounds on the target correlation are computed, and it is shown that very large positive or negative correlations may not be able to be simulated using the translation model. The correlation distortion function is shown to be odd if either of the inverse cdfs of the individual components is odd.

Three illustrative examples are given. In the first, a two-dimensional random vector with one component exponentially distributed and one cubic is shown to have significant correlation distortion. In the second, the crystallographic orientation of an aluminum alloy is modelled as a random vector of the Euler angles. Attempts to simulate this random vector using translation models illustrate the possibility of matching target marginal distributions and second moment properties of real experimental data, while only approximately matching the joint distribution of the target random vector. The match to the target joint distribution is poor, demonstrating a key liability of second moment characterization of non-Gaussian random quantities. Lastly, the correlated elasticity and viscosity constants of an F-Actin gel are successfully modelled using the translation transformation. By way of closing, an outline is given of a method currently being developed to simulate non-stationary, non-Gaussian random processes using translation models.

Acknowledgements

The author gratefully acknowledges valuable input from M. Grigoriu. D.P. Mika, Y. Tseng, and D. Wirtz graciously provided the data used in this study.

References

[1] Deodatis G, Micaletti R. Simulation of highly skewed non-Gaussian stochastic processes. J Engng Mech, ASCE 2001; 127(12):1284–95.
[2] Gurley K, Kareem A. Analysis, interpretation, modeling and simulation of unsteady wind and pressure data. J Wind Engng Ind Aerodyn 1997;657–69.
[3] Sakamoto S, Ghanem R. Polynomial chaos decomposition for the simulation of non-Gaussian non-stationary stochastic processes. J Engng Mech 2002;128:190–201.
[4] Gurley KR, Kareem A, Tognarelli MA. Simulation of a class of non-normal random processes. Int J Non-linear Mech 1996;31: 601–17.
[5] Grigoriu M. Crossing of non-Gaussian translation processes. J Engng Mech, ASCE 1984;110(4):610–20.
[6] Grigoriu M, Ditlevsen O, Arwade SR. A Monte Carlo simulation model for stationary non-Gaussian processes. Probab Engng Mech 2003;18:87–95.
[7] Gioffre M, Gusella V, Grigoriu M. Simulation of non-Gaussian field applied to wind pressure fluctuations. Probab Engng Mech. 2000;15:339–45.
[8] Deutsch R. Nonlinear transformations of random processes. Englewood Cliffs, NJ: Prentice Hall; 1962.
[9] Dawson PR. Computational crystal plasticity. Int J Solids Struct 2000; 37:115–30.
[10] Acharjee S, Zabaras N. A proper orthogonal decomposition approach to microstructure model reduction in rodrigues space with applications to optimal control of microstructure-sensitive properties. Acta Materialia 2003;51:5627–46.
[11] Arwade SR, Grigoriu M. Evolution of crystallographic orientations in crystals subject to random and deterministic deformation. Probab Engng Mech 2003;18:289–99.

[12] Arwade SR, Grigoriu M. A probabilistic model for polycrystalline microstructures with application to intergranular fracture. ASCE J Engng Mech 2004;130:997–1005.
[13] Bunge H-J. Texture analysis in materials science. London: Butterworths; 1982.
[14] Mika D. Personal communication; 1997.
[15] Apgar J, Tseng Y, Fedorova E, Herwig MB, Almo SC, Wirtz D. Multiple-particle tracking measurements of heterogeneities in solutions of actin filaments and actin bundles. Biophys J 2000;79: 1095–106.
[16] Tseng Y, Kole TP, Lee S-H, Wirtz D. Local dynamics and viscoelastic properties of cell biological systems. Curr Opin Colloidal Interface Sci 2002;7:210–7.
[17] Phoon K, Huang SP, Quek ST. Simulation of second-order processes using karhunen–loeve expansion. Comput Struct 2002;80: 1049–60.
[18] Spanos PD, Rao VRS. Random field representation in a biorthogonal wavelet basis. ASCE J Engng Mech 2001;127:194–205.
[19] Spanos P, Failla G. Evolutionary spectra estimation using wavelets. ASCE J Engng Mech 2004;130:952–60.